DATA ANALYSIS AND CLASSICAL ESTIMATION METHODS OF THE BOUNDED POWER LOMAX DISTRIBUTION

Amal S. Hassan [1], Asma M. Khalil [2] and Heba F. Nagy [3,*]

1 Faculty of Graduate Studies for Statistical Research, Cairo University, 12613, Giza, Egypt: amal52_soliman@cu.edu.eg
2 Faculty of Graduate Studies for Statistical Research, Cairo University, 12613, Giza, Egypt: 12422020463929@pg.cu.edu.eg
3 Faculty of Graduate Studies for Statistical Research, Cairo University, 12613, Giza, Egypt: heba_nagy_84@cu.edu.eg
* **Correspondence:** Email: heba_nagy_84@cu.edu.eg

Abstract

In this work, a novel bounded three-parameter power Lomax distribution termed the unit power Lomax (UPLoD) is presented. The UPLoD is capable of handling data with left and right skewed shapes according to its probability density function. Additionally, according to the hazard rate function, the distribution may be used to analyse data containing J-shaped hazard rates. It is possible to determine some of the distribution's mathematical characteristics like moments, probability-weighted moments, incomplete moments, residual and reversed residual life, quantile function, stress strength model, and entropy (Rényi, Havrda and Charvát, Tsallis, and Arimoto) measures. The Cramér–von Mises, weighted least squares, maximum likelihood, Anderson–Darling, maximum product of spacing, and least squares approaches are among the conventional estimating techniques that are taken into account. The performance of the resulting estimates is compared using a Monte Carlo simulation based on some precision metrics. An actual data application is presented using water capacity data, and data about the Susquehanna River's maximum flood levels to show the importance of the new distribution compared to several other known distributions.

Keywords: Unit Power Lomax distribution, Entropy measures, Parameter estimation, Goodness-of-fit test.

1 Introduction

The Lomax distribution (LoD), sometimes referred to as the Pareto II distribution, was first presented by Lomax [1] to model business failure data, but it has since been widely used in a wide range of applications. Harris [2] utilized the LoD for data on wealth and income, In the case of severely tailed data, Bryson [3] suggested employing it in place of the exponential distribution. Atkinson and Harrison [4] used it to model data on business failure. It was utilized in the biological sciences and even for modeling the distribution of server computer file sizes, as mentioned by Holland *et al.* [5]. The LoD has been used to model a variety of data that many writers have explored.

Rady *et al.* [6] presented the power Lomax distribution (PLoD) as a generalization of the LoD that includes an additional shape parameter. The PLoD has been used in many applications and fields, like

those pertaining to biological sciences, engineering sciences, medical research, econometrics, and life testing. The PLoD's probability density function (PDF) is provided by:

$$f\left(x;\omega\right)=\kappa\tau^{-1}\eta x^{\kappa-1}\left(1+\tau^{-1}x^{\kappa}\right)^{-\eta-1};x>0, \tag{1}$$

where $\omega=(\kappa,\eta,\tau)$ is the set of parameters, $\kappa>0$ and $\eta>0$ are shape parameters and $\tau>0$ is the scale parameter. The following defines the PLoD's cumulative distribution function (CDF)

$$F\left(x;\omega\right)=1-\left(1+\frac{x^{\kappa}}{\tau}\right)^{-\eta};x>0. \tag{2}$$

On the other hand, statistics professionals have recently become interested in the creation and the development of novel probability distributions that can provide models that fit datasets ranging from zero to one. To model proportions, percentages, and probabilities, bounded distributions are required. The study of datasets on (0, 1) regard to parametric or semi-parametric regression models is crucial in applied fields. Additionally, unit distributions add more flexibility over the course of the unit interval without changing the core distribution's properties. When modeling proportions that are typically seen in industry, medical applications, and risk analysis, unit distributions are an essential tool.

Here are a few of the most significant unit distributions with varying numbers of parameters. The log Lindley distribution (Gómez-Déniz *et al.* [7]), unit-Gompertz distribution(UGoD) (Mazucheli *et al.* [8]), unit Lindley distribution (ULD) (Mazucheli *et al.* [9]), unit modified Burr-III distribution (Haq *et al.* [10]), unit generalized half normal distribution (Korkmaz [11]), unit-Weibull distribution (UWD) (Mazucheli *et al.* [12]), unit Gamma/Gompertz distribution (UG/GD) (Bantan *et al.* [13]), unit log logistic distribution (ULLD) Ribeiro-Reis [14]), unit Burr-XII distribution (UBXIID) (Korkmaz and Chesneau [15]), unit half-logistic geometric distribution (Ramadan *et al.* [16]), unit power-skew-normal distribution (Martínez-Flórez *et al.* [17]), unit exponentiated half logistic distribution (Hassan *et al.* [18]), unit Teissier distribution (Krishna *et al.* [19]), unit Xgamma distribution (Hashmi *et al.* [20]), unit-exponentiated Pareto distribution (UEPD) (Haj Ahmad *et al.* [21]), unit exponentiated Lomax (Fayomi *et al.* [22]), Kumaraswamy unit-Gompertz distribution (Akata *et al.* [23]), unit inverse exponentiated Weibull distribution (Hassan and Alharbi [24]) and unit–power Burr X distribution (Fayomi *et al.* [25]).

The main goal of this work is to present a new and adaptable probabilistic model for the PLoD with a domain (0,1). This model refers to the unit PLoD (UPLoD) that can be used to evaluate a wide range of data sets with values ranging from zero to one. The UPLoD is presented in light of the following details:

a) To offer a new distribution that is specified on (0,1) to compete with the current bounded distributions.
b) There are several possible forms for the density function: symmetric, unimodal, reversed J-shaped, left- and right-skewed. Furthermore, J-shaped and rising hazard rate function (HF) plots of the UPLoD are possible.
c) Statistical characteristics are given, including quantile function, stress strength (SS) reliability model, moments, incomplete moments (IMs), probability-weighted moments (PWMs), residual and inverted residual lives, and entropy measures.
d) The performance of parameter estimate for the UPLoD is assessed and compared using six traditional estimation techniques: least squares (LS), weighted LS (WLS), maximum likelihood (ML), maximum product spacing (MPS), Anderson-Darling (AD), and Cramer-von Mises (CvM).
e) To evaluate the validity of different estimates, simulation research is conducted. The Susquehanna River's maximum flood level and water capacity data are used to evaluate the UPLoD's usefulness to a number of alternative models.

The structure of the article is as follows: A new bounded distribution is shown in Section 2. In Section 3, the statistical characteristics of the UPLoD are covered. The model parameter estimators based on ML, LS, CvM, WLS, AD, and MPS methods are derived in Section 4. In order to make sense of the findings in Section 5, a simulation study is conducted. In Section 6, two real data sets are used to demonstrate the UPLoD's utility. Section 7 presents the conclusions.

2 Unit Power Lomax Distribution

In this section, a new lifetime model called the UPLoD is introduced and investigated. The UPLoD is obtained by using the exponential function transformation in the form $Y = e^{-X}$ where X has the PLoD with density function (1), hence the UPLoD's PDF is provided by:

$$f(y;\omega) = \frac{\kappa\eta}{\tau y}(-\ln y)^{\kappa-1}\left(1+\tau^{-1}(-\ln y)^{\kappa}\right)^{-\eta-1};\ 0<y<1;\ \kappa,\eta,\tau>0, \tag{3}$$

where $\omega = (\kappa,\eta,\tau)$ is the set of parameters, where κ and η are shape parameters, while τ is scale parameter. The CDF of the UPLoD is provided as follows:

$$F(y;\omega) = \left(1+\tau^{-1}(-\ln y)^{\kappa}\right)^{-\eta},\quad 0<y<1. \tag{4}$$

The survival and HF of the UPLoD, for 0< y <1, are given, in that order, by

$$S(y;\omega) = 1-\left(1+\tau^{-1}(-\ln y)^{\kappa}\right)^{-\eta},$$

and,

$$h(y;\omega) = \frac{\eta\kappa(-\ln y)^{\kappa-1}\left(1+\tau^{-1}(-\ln y)^{\kappa}\right)^{-\eta-1}}{\tau y\left[1-\left(1+\tau^{-1}(-\ln y)^{\kappa}\right)^{-\eta}\right]}.$$

Figure 1 represents the PDF plots of the UPLoD for selected parameter values. It shows that the UPLoD exhibits symmetric, unimodal, reversed J-shaped, left-skewed and right-skewed shapes. Also, the HF plots of UPLoD for some values of parameters are increasing and J-shaped.

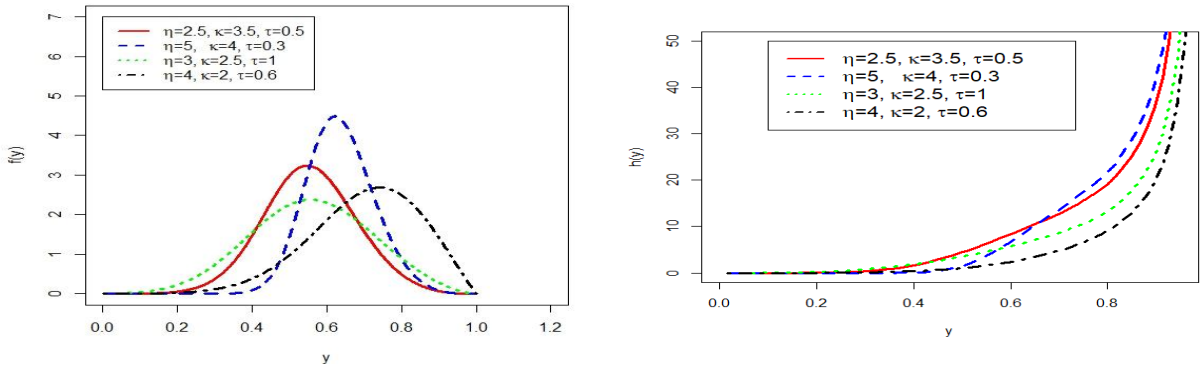

Figure 1: *Plots of the PDF and HF for the UPLoD*

The quantile function of a random variable Y has the UPLoD is obtained. The quantile function of the UPLoD, say $y = Q(p) = F^{-1}(p)$, where p~ uniform (0,1) can be obtained by inverting CDF (4) as follows:

$$p = \left[1+\tau^{-1}(-\ln y)^{\kappa}\right]^{-\eta}.$$

Then, the quantile function of the UPLoD takes the following form

$$Q(p) = e^{-\tau^{1/\kappa}\left((p)^{-1/\eta}-1\right)^{1/\kappa}}. \quad (5)$$

The first quantile (Q_1) is obtained by setting $p = 0.25$ in (5); the median (Q_2) is obtained by setting $p = 0.5$ in (5); and the third quantile (Q_3) is obtained by setting $p = 0.75$ in (5).

3 Some Statistical Properties

In this section, some statistical properties of the UPLoD, including, the r^{th} moment, PWMs, IMs, and moments of residual, some entropy measures, and SS reliability are derived.

3.1 Moments & Some Measures

Ordinary moments can be used to gain a large number of a UPLoD's significant properties and attributes. It is simple to extract the UPLoD's r^{th} moment from PDF (3) in the manner that follows

$$E(Y^r) = \int_0^1 \frac{\eta\kappa}{\tau y} y^r (-\ln y)^{\kappa-1}\left(1+\tau^{-1}(-\ln y)^{\kappa}\right)^{-\eta-1} dy$$

$$= \sum_{h=0}^{\infty} A_h(\omega) B\left(\frac{h}{\kappa}+1, \eta-\frac{h}{\kappa}\right); \eta > \frac{h}{\kappa},$$

where $A_h(\omega) = \frac{(-r)^h \eta \tau^{h/\kappa}}{h!}$ and $B(.,.)$ is the Beta function. Certain numerical values of mean (μ_1'), variance (σ^2), skewness (α_3), kurtosis (α_4) and coefficient of variation (CV) are mentioned in Table 1 for some selected parameter values.

Table 1: *Some moments measures of the UPLoD*

τ	η	κ	μ_1'	σ^2	CV	α_3	α_4
1	0.7	7	0.337	0.011	0.031	-0.113	3.317
	0.9	9	0.361	0.006	0.015	-0.049	3.709
	1.1	11	0.373	0.003	0.009	0.093	3.853
2	0.7	7	0.302	0.010	0.034	0.009	3.280
	0.9	9	0.333	0.006	0.016	0.022	3.684
	1.1	11	0.350	0.003	0.0095	0.137	3.859
3	0.7	7	0.283	0.009	0.035	0.084	3.285
	0.9	9	0.317	0.005	0.017	0.066	3.679
	1.1	11	0.337	0.003	0.0097	0.164	3.866

Table 1 indicates that when the values of η and κ rises while the value of τ remain constant, the values of σ^2 and CV fall and the values of the other measures increase. It is therefore possible to draw the conclusion that, as the value of τ rises for predetermined values of η and κ, then the values of the mean and variance decrease, while the values of other measures increase. Thus, it can be claimed that the distribution is skewed to right and left, according to the values of skewness. Finally, according to values of α_4 in Table 1, the UPLoD is leptokurtic.

i. The probability-Weighted Moments

It was Greenwood *et al.* [26] who proposed the PWM. Estimators of parameters and the quantile function of the generalized distributions expressible in inverse form are derived using the PWM. Given two positive integers, *s* and *r*, the PWM of a random variable Y is defined as

$$\nu_{s,r} = \int_{-\infty}^{\infty} y^s \left[F(y)\right]^r f(y)\, dy. \tag{6}$$

Using PDF (3) and CDF (4) in (6), the PWM of the UPLoD is derived as follows

$$\nu_{s,r} = \frac{\eta\kappa}{\tau}\int_0^1 y^{s-1}\left(-\ln y\right)^{\kappa-1}\left(1+\tau^{-1}\left(-\ln y\right)^{\kappa}\right)^{-\eta(r+1)-1} dy$$

$$= \sum_{h=0}^{\infty} \frac{(-1)^h s^h (\tau)^{\frac{h}{\kappa}} \eta}{h!} B\left(\frac{h}{\kappa}+1, \eta(r+1)-\frac{h}{\kappa}\right).$$

ii. The incomplete Moments

Understanding a distribution's form as well as its mean is vital for the solutions to many important economic concerns. This is made clear throughout the study of econometrics (for instance, asymmetric error terms cannot continue to be produced by the widely held spherical distributions). The r^{th} IM of the UPLoD is obtained as follows by utilizing PDF (3)

$$\phi_r(x) = \frac{\eta\kappa}{\tau}\int_0^x y^{r-1}\left(-\ln y\right)^{\kappa-1}\left(1+\tau^{-1}\left(-\ln y\right)^{\kappa}\right)^{-\eta-1} dy$$

$$= \sum_{h=0}^{\infty} A_h(\omega)\, \mathrm{B}\left(\frac{h}{\kappa}+1, \eta-\frac{h}{\kappa}, \left(1+\frac{(-\ln x)^{\kappa}}{\tau}\right)^{-1}\right),$$

where B(.,.,x) is incomplete Beta function.

iii. Residual and Reversed Residual Life's

Residual life and reversed residual life random variables are often used in risk analysis. As a result, Balkema and De Haan [27] looked into some related statistical functions, including the survival function, mean, and variance. The residual life is defined as the interval between time t and the time of failure for the conditional random variable. The r^{th} moment of the residual life, say $I_r(t)$ is defined as follows:

$$I_r(t) = \frac{1}{S(t)}\sum_{n=0}^{r}\int_t^{\infty}(y-t)^r f(y)\, dy = \frac{1}{S(t)}\sum_{n=0}^{r}\binom{r}{n}(-t)^{r-n}\int_t^{\infty} y^n f(y)\, dy. \tag{7}$$

Additionally, by combining PDF (3) into (7), the r^{th} moment of residual life of the UPLoD can be obtained as follows:

$$I_r(t) = \frac{1}{S(t;\omega)}\sum_{n=0}^{r}\binom{r}{n}(-t)^{r-n}\int_t^1 \frac{\eta\kappa}{\tau} y^{n-1}(-\ln y)^{\kappa-1}\left(1+\tau^{-1}(-\ln y)^{\kappa}\right)^{-\eta-1} dy.$$

After some manipulation, $I_r(t)$ takes the following form

$$I_r(t) = \frac{1}{S(t;\omega)}\sum_{n=0}^{r} l_{h,n}\, \mathrm{B}\left(\frac{h}{\kappa}+1, \eta-\frac{h}{\kappa}, \left(1+\tau+(-\ln t)^{-\kappa}\right)^{-1}\right),$$

where $l_{h,n} = (-t)^{r-n}\binom{r}{n}\sum_{j=0}^{\infty}\frac{(-1)^h n^h \tau^{\frac{h}{\kappa}}\eta}{h!}$.

Further, the r^{th} moment of reversed residual life of the UPLoD is derived as follows:

$$\varepsilon_r(t)=\frac{1}{F(t)}\sum_{n=0}^{r}\int_{t}^{\infty}(t-y)^r\, f(y)\, dy$$

$$=\frac{1}{F(t;\omega)}\sum_{n=0}^{r}(-1)^n\binom{r}{n}t^{r-n}\int_{0}^{t}\frac{\eta\kappa}{\tau}y^{n-1}(-\ln y)^{\kappa-1}\left(1+\tau^{-1}(-\ln y)^{\kappa}\right)^{-\eta-1}dy,$$

which is the incomplete beta function, and takes the following form

$$\varepsilon_r(t)=\frac{1}{F(t;\omega)}\sum_{n=0}^{r}l'_{h,n}\,\mathrm{B}\left(\frac{h}{\kappa}+1,\eta-\frac{h}{\kappa},\left(1+\tau^{-1}(-\ln x)^{\kappa}\right)^{-1}\right),$$

where $l'_{h,n}=(-1)^n t^{r-n}\binom{r}{n}\sum_{h=0}^{\infty}\frac{(-1)^h n^h \tau^{\frac{h}{\kappa}}\eta}{h!}$.

3.2 Some Entropy measures

In research on reliability and risk assessment, entropy measures are essential. It has been used in many biological applications and in the physical and medical domains. Entropy measures how much the uncertainty associated with a random variable Y's distribution fluctuates. Some entropy measures of the UPLoD as Rényi, Havrda and Charvat, Tsallis and Arimoto are obtained here.

The Rényi entropy, of order $\gamma>0$ and $\gamma\neq 1$, for the UPLoD is defined by:

$$R_\gamma=\frac{1}{1-\gamma}\log\left[\int_{-\infty}^{\infty}f(y)^\gamma dy\right]. \tag{8}$$

The Rényi entropy of the UPLoD is obtained by using PDF (3) in (8) as follows:

$$R_\gamma=(1-\gamma)^{-1}\log\left[\left(\frac{\eta\kappa}{\tau}\right)^{\gamma}\int_{0}^{1}(-\ln y)^{\gamma(\kappa-1)}y^{-\gamma}\left(1+\tau^{-1}(-\ln y)^{\kappa}\right)^{-\gamma(\eta+1)}dy\right].$$

Hence, the Rényi entropy of the UPLoD takes the following form

$$R_\gamma=(1-\gamma)^{-1}\log\left[\sum_{h=0}^{\infty}\delta_h(\omega,\gamma)B\left(\frac{h-\gamma+1}{\kappa}+\gamma,\gamma\eta-\frac{(h-\gamma+1)}{\kappa}\right)\right],$$

where $\delta_h(\omega,\gamma)=\frac{\kappa^{\gamma-1}\eta^{\gamma}(\gamma-1)^h\tau^{\kappa^{-1}(h-\gamma+1)}}{h!}$.

Shannon's entropy was extended by Havrda and Charvát [28]. Havrda and Charvat (HC) of the UPLoD is obtained from PDF (3) as follows

$$HC_\gamma=\frac{1}{2^{1-\gamma}-1}\left[\int_{0}^{1}\left(\frac{\eta\kappa}{\tau y}\right)^{\gamma}(-\ln y)^{\gamma(\kappa-1)}\left(1+\tau^{-1}(-\ln y)^{\kappa}\right)^{-\gamma(\eta+1)}dy-1\right].$$

Using the same procedure in Rényi entropy, then, the UPLoD's HC entropy has the following structure.

$$HC_\gamma=\frac{1}{2^{1-\gamma}-1}\left[\left[\sum_{h=0}^{\infty}\delta_h(\omega,\gamma)B\left(\gamma+\frac{h-\gamma+1}{\kappa},\gamma\eta-\frac{(h-\gamma+1)}{\kappa}\right)\right]^{\frac{1}{\gamma}}-1\right].$$

Tsallis [29] proposed an extension of Shannon's entropy. Tsallis entropy of the UPLoD is acquired as follows from PDF (3)

$$T_\gamma = (\gamma-1)^{-1}\left[1-\left(\frac{\eta\kappa}{\tau}\right)^{\gamma}\int_0^1(-\ln y)^{\gamma(\kappa-1)}y^{-\gamma}\left(1+\tau^{-1}(-\ln y)^{\kappa}\right)^{-\gamma(\eta+1)}dy\right].$$

By the similar way used above, hence the UPLoD's Tsallis entropy has the following structure

$$T_\gamma = \frac{1}{\gamma-1}\left[1-\sum_{h=0}^{\infty}\delta_h(\omega,\gamma)B\left(\gamma+\frac{h-\gamma+1}{\kappa},\ \gamma\eta-\frac{(h-\gamma+1)}{\kappa}\right)\right].$$

An alternative entropy metric with comparable qualities to the Shannon entropy measure was proposed by Arimoto [30] and named the Arimoto's entropy. The following is how to derive Arimoto's entropy of the UPLoD from PDF (3).

$$A_\gamma = \frac{\gamma}{1-\gamma}\left[\left(\int_0^1\left(\frac{\eta\kappa}{\tau y}\right)^{\gamma}(-\ln y)^{\gamma(\kappa-1)}\left(1+\tau^{-1}(-\ln y)^{\kappa}\right)^{-\gamma(\eta+1)}dy\right)^{1/\gamma}-1\right].$$

In the same vein used above, the UPLoD's Arimoto's entropy has the following structure

$$A_\gamma = \frac{\gamma}{1-\gamma}\left[\left[\sum_{h=0}^{\infty}\delta_h(\omega,\gamma)B\left(\gamma+\frac{h-\gamma+1}{\kappa},\ \gamma\eta-\frac{(h-\gamma+1)}{\kappa}\right)\right]^{1/\gamma}-1\right].$$

Certain numerical values of some entropy measures of the UPLoD are mentioned in Table 2 for some predetermined values of the parameters.

Table 2: *A selection of entropy measures of the UPLoD*

γ	τ	η	κ	R_γ	T_γ	HC_γ	A_γ
0.3	0.5	0.5	1	-0.1550	-0.1469	0.2675	0.1301
		2	2	-0.1168	-0.1122	0.2043	0.1023
		5	3	-0.5033	-0.4242	0.7724	0.2961
		7	4	-0.6937	-0.5495	1.0006	0.3436
		9	5	-0.8420	-0.6362	1.1584	0.3685
		11	6	-0.9676	-0.7029	1.2799	0.3837
0.5		0.5	1	-0.3397	-0.3125	0.5334	0.2880
		2	2	-0.1780	-0.1703	0.2908	0.1631
		5	3	-0.6263	-0.5377	0.9179	0.4654
		7	4	-0.8295	-0.6790	1.1591	0.5637
		9	5	-0.9916	-0.7818	1.3347	0.6290
		11	6	-1.1300	-0.8633	1.4737	0.6770
0.8		0.5	1	-1.1101	-0.9955	1.5380	0.9694
		2	2	-0.2502	-0.2440	0.3770	0.2425
		5	3	-0.7354	-0.6839	1.0566	0.6718
		7	4	-0.9504	-0.8655	1.3372	0.8459
		9	5	-1.1235	-1.0062	1.5546	0.9795
		11	6	-1.2709	-1.1222	1.7339	1.0888

Table 2 indicates that when the values of γ increases while the value of $\eta,\kappa,\tau,$ remain constant the values of the T_γ and R_γ decrease and values of the other measures increase. Consequently, it can be deduced that when the value of η and κ grow for constant values of τ and γ, then the values of the T_γ and R_γ fall and values of the other measures rise.

3.3 Stress-Strength Reliability

The SS model, say $R = P[Y < X]$, where X is the strength and Y is the stress of the system, is widely used in several fields such as engineering, statistics, and biostatistics. A few real-world examples include buildings, the deterioration of rocket engines, the aging of concrete pressure vessels, and the fatigue failure of aircraft structures. For more applications and examples (see [31-33]). Assume that X be the system's strength and Y stress, where X and Y are independent random variables having UPLoD (κ, η_1, τ) and UPLoD (κ, η_2, τ), respectively, then the SS reliability is given as follows

$$R = \int_{y=0}^{1} \int_{x=0}^{y} \frac{\kappa\eta_2}{\tau x}(-\ln x)^{\kappa-1}\left(1+\tau^{-1}(-\ln x)^{\kappa}\right)^{-\eta_2-1} \frac{\kappa\eta_1}{\tau y}(-\ln y)^{\kappa-1}\left(1+\tau^{-1}(-\ln y)^{\kappa}\right)^{-\eta_1-1} dx\, dy.$$

Hence, the stress strength of the UPLoD takes the following form

$$R = \frac{\eta_1}{(\eta_1+\eta_2)}.$$

4 Parameter Estimation

In this section, six different estimation methods for estimating model parameters are presented. These methods are ML, LS, WLS, CvM, AD and MPS.

4.1 Maximum Likelihood Estimator

The estimation of the UPLoD parameters is deemed using the ML method. Let $y_1, y_2 \ldots y_m$ be a random sample of size m from the UPLoD, the log-likelihood function, pointed by $\ln M^*$, is given by

$$\ln M^* = m\ln(\eta) + m\ln(\kappa) - m\ln(\tau) - \sum_{r=1}^{m} \ln y_r + (\kappa-1)\sum_{r=1}^{m} \ln(-\ln y_r)$$

$$-(\eta+1)\sum_{r=1}^{m} \ln\left(1+\tau^{-1}(-\ln y_r)^{\kappa}\right).$$

An alternative to previous equation, we obtain the ML equations as below:

$$\frac{\partial \ln M^*}{\partial \eta} = \frac{m}{\eta} - \sum_{r=1}^{m}\left(1+\frac{1}{\tau}(-\ln y_r)^{\kappa}\right),$$

$$\frac{\partial \ln M^*}{\partial \tau} = \frac{-m}{\tau} + \sum_{r=1}^{m} \frac{(\eta+1)}{\tau^2(-\ln y_r)^{-\kappa}+\tau},$$

and

$$\frac{\partial \ln M^*}{\partial \kappa} = \frac{m}{\kappa} + \sum_{r=1}^{m} \ln(-\ln y_r) - \sum_{r=1}^{m} \frac{(\eta+1)\ln(-\ln y_r)}{\left(1+\tau(-\ln y_r)^{-\kappa}\right)}.$$

By numerically solving $\partial \ln M^*/\partial\eta = 0$, $\partial \ln M^*/\partial\tau = 0$, and $\partial \ln M^*/\partial\kappa = 0$, based on optimization algorithm as optim using R program, the ML estimates (MLEs) of η, τ, and κ are produced.

4.2 Least Squares & Weighted Least Squares

Let $y_1, y_2, \ldots, y_m$ be a random sample of size m from the UPLoD. Suppose that $y_{(1)} < y_{(2)} < \ldots < y_{(m)}$ denotes the corresponding ordered sample. Minimizing the sum squares error yields the LS and WLS estimators of the unknown parameters of the UPLoD.

$$l^*(\omega)=\sum_{r=1}^{m}\vartheta_r\left[\left(1+\frac{1}{\tau}(-\ln y_{(r)})^{\kappa}\right)^{-\eta}-\frac{r}{m+1}\right]^2. \tag{9}$$

Alternatively, the LS estimates (LSEs) of η,τ,κ, can be obtained by setting $\vartheta_r=1$ in (9). Similarly, the WLS estimates (WLSEs) of unknown parameters are obtained from (9) by putting $\vartheta_r=\frac{(m+1)^2(m+2)}{r(m-r+1)}$. These estimates can also be obtained by solving the following non-liner equations using an optimization algorithm

$$\frac{\partial l^*(\omega)}{\partial\tau}=\sum_{r=1}^{m}\vartheta_r\left[\left(\left(\tau^{-1}(-\ln y_{(r)})^{\kappa}\right)+1\right)^{-\eta}-\frac{r}{m+1}\right]\Im_1(y_{(r)}\mid\omega)=0,$$

$$\frac{\partial l^*(\omega)}{\partial\eta}=\sum_{r=1}^{m}\vartheta_r\left[\left(\left(\tau^{-1}(-\ln y_{(r)})^{\kappa}\right)+1\right)^{-\eta}-\frac{r}{m+1}\right]\Im_2(y_{(r)}\mid\omega)=0,$$

and,

$$\frac{\partial l^*(\omega)}{\partial\kappa}=\sum_{r=1}^{m}\vartheta_r\left[\left(\left(\tau^{-1}(-\ln y_{(r)})^{\kappa}\right)+1\right)^{-\eta}-\frac{r}{m+1}\right]\Im_3(y_{(r)}\mid\omega)=0,$$

where,

$$\Im_1(y_{(r)}\mid\omega)=\frac{\partial\left[\left((\tau^{-1}(-\ln y_{(r)})^{\kappa})+1\right)^{-\eta}\right]}{\partial\tau}=\eta\tau^{-2}(-\ln y_{(r)})^{\kappa}\left(1+\tau^{-1}(-\ln y_{(r)})^{\kappa}\right)^{-\eta-1},$$

$$\Im_2(y_{(r)}\mid\omega)=\frac{\partial\left[\left((\tau^{-1}(-\ln y_{(r)})^{\kappa})+1\right)^{-\eta}\right]}{\partial\eta}=-\left(1+\tau^{-1}(-\ln y_{(r)})^{\kappa}\right)^{-\eta}\ln\left(1+\tau^{-1}(-\ln y_{(r)})^{\kappa}\right), \tag{10}$$

$$\Im_3(y_{(r)}\mid\omega)=\frac{\partial\left[\left((\tau^{-1}(-\ln y_{(r)})^{\kappa})+1\right)^{-\eta}\right]}{\partial\kappa}$$

$$=-\eta\tau^{-1}(-\ln y_{(r)})^{\kappa}\ln(-\ln y_{(r)})\left(1+\tau^{-1}(-\ln y_{(r)})^{\kappa}\right)^{-\eta-1}.$$

4.3 Maximum Product Spacing

The ML approach can be replaced by the MPS method, which approaches the Kullback-Leibler information metric. Although ML estimation is the most popular and extensively used approach, it does not work well in some situations involving big samples and complex continuous distributions. The spacing between the values of the CDF at consecutive data points is the foundation of the MPS approach. The MPS has been used in several applications such as pure mathematics, statistics, hydrology, econometrics, magnetic resonance imaging and others. Let $Y_{(1)}<Y_{(2)}<\ldots<Y_{(m)}$ be the ordered statistics from the distribution with sample size m, and $y_{(1)}<y_{(2)}<\ldots<y_{(m)}$ be the ordered observed values. Cheng and Amin [34] introduced the MPS method serving as an alternative to the ML method.

Let $y_{(1)}<y_{(2)}<\ldots<y_{(m)}$ are ordered random samples from the UPLoD having CDF(4). The uniform spacings can be defined as follows, based on a size m random sample from the UPLoD.

$$D_r(\omega)=F\left(y_{(r)}|\omega\right)-F\left(y_{(r-1)}|\omega\right),\ r=1,2,...,m+1,$$

where, $F\left(y_{(0)}|\omega\right)=0,\ F\left(y_{(m+1)}|\omega\right)=1$ and $\sum_{r=1}^{m+1} D_r(\omega)=1$.

The MPS estimate (MPSE) for the UPLoD is given by maximizing the geometric mean of the spacings

$$S^*(\omega)=\frac{1}{1+m}\sum_{r=1}^{m+1}\ln D_r(\omega)=\frac{1}{1+m}\sum_{r=1}^{m+1}\ln\left[\left(1+\tau^{-1}\left(-\ln y_{(r)}\right)^{\kappa}\right)^{-\eta}-\left(1+\tau^{-1}\left(-\ln y_{(r-1)}\right)^{\kappa}\right)^{-\eta}\right].$$

The MPSE of $\eta,\tau,$ and κ are obtained by solving the following non-liner equations technique

$$\frac{\partial S^*(\omega)}{\partial\tau}=\frac{1}{1+m}\sum_{r=1}^{m+1}\left[\frac{\Im_1(y_{(r)}\,|\,\omega)-\Im_1(y_{(r-1)}\,|\,\omega)}{D_r(\omega)}\right]=0,$$

$$\frac{\partial S^*(\omega)}{\partial\eta}=\frac{1}{1+m}\sum_{r=1}^{m+1}\left[\frac{\Im_2(y_{(r)}\,|\,\omega)-\Im_2(y_{(r-1)}\,|\,\omega)}{D_r(\omega)}\right]=0,$$

and,

$$\frac{\partial S^*(\omega)}{\partial\kappa}=\frac{1}{1+m}\sum_{r=1}^{m+1}\left[\frac{\Im_3(y_{(r)}\,|\,\omega)-\Im_3(y_{(r-1)}\,|\,\omega)}{D_r(\omega)}\right]=0,$$

where $\Im_k(y_{(r)}\,|\,\omega)$, k =1, 2 and 3 are given in Equation (10). Also, $\Im_k(y_{(r-1)}\,|\,\omega)$, k =1, 2 and 3 are given in (10) by replacing (r) with (r–1).

4.4 Cramer-von Mises & Anderson-Dalring Estimators

The CvM estimates (CvMEs) and AD estimates (ADEs) of set parameters of $\omega=(\eta,\kappa,\tau),$ are obtained by minimizing the following functions:

$$C(\omega)=\frac{1}{12m}+\sum_{r=1}^{m}\left[\left(1+\tau^{-1}(-\ln y_{(r)})^{\kappa}\right)^{-\eta}-\frac{2r-1}{2m}\right]^2,$$

and,

$$\mathrm{A}^{\bullet}(\omega)=-m-\sum_{r=1}^{m}\frac{2r-1}{m}\left[\left[\ln\left(1+\tau^{-1}(-\ln y_{(r)})^{\kappa}\right)^{-\eta}\right]+\ln\left[1-\left(1+\tau^{-1}(-\ln y_{(\mathrm{m}+1-r)})^{\kappa}\right)^{-\eta}\right]\right],$$

with respect to τ,η and κ.

5 Numerical Study

In this section, a numerical analysis was conducted to assess and compare the performance of the estimates with regard to their relative absolute biases (RAB), chosen parameter values and mean squared errors (MSEs) for different sample sizes. The following steps provide a description of the numerical techniques:

Step 1: A random sample is created from the UPLoD by using the inverse transformation (5) with sample sizes m = (50, 75, 100, 125, 150, and 175).

Step 2: Some parameter values are selected as, **Set1:** $(\eta=2,\kappa=0.8,\tau=0.05)$, **Set2:** $(\eta=2.5,\kappa=0.8,\tau=0.05)$, **Set3:** $(\eta=3,\kappa=0.67,\tau=0.05)$, **Set4:** $(\eta=3.5,\kappa=0.67,\tau=0.05)$, **Set5:** $(\eta=3,\kappa=0.8,\tau=0.05)$, and **Set 6:** $(\eta=3.5,\kappa=0.8,\tau=0.05)$.

Step 3: Obtain the parameter estimates of η,κ,τ using the provided estimation methods for the selected sample sizes.

Step 4: Steps 1 through 4 are repeated 1000 times for each sample size and the chosen parameter values. Then, the MSEs and RABs of different estimates of η, κ, τ are computed. The MSEs and RABs have the following formulas

$$RAB(\omega) = \frac{1}{1000}\sum_{k=1}^{1000}\left|\frac{\hat{\omega}_k - \omega_k}{\omega_k}\right|, \quad MSE(\omega) = \frac{1}{1000}\sum_{k=1}^{1000}\left(\hat{\omega}_k - \omega_k\right)^2.$$

Step 5: The numerical results of the simulation study are listed in Tables (3–8).

The findings obtained regarding the behavior of the estimated parameters from the UPLoD are as follows:

1. The RABs of all estimates decrease with increasing sample sizes based on different estimation techniques (see Tables (3–8)).
2. The MSEs for the η estimate increase as value of η increases and the MSEs for the κ estimate decrease as the value of η increases, for all estimation methods (see Tables 3, 7 and 8).
3. From Tables 5 and 7 it is observed that the RAB of κ estimate generally increase and the RAB of η estimate generally decrease when κ increases for all estimation methods.
4. From Tables 4 and 8 it is observed that the RAB of η, κ estimates generally constant when η increases for all estimation methods.
5. The RAB of τ estimate generally decreases when κ and η increase.
6. For all selected sets of parameters, the MSEs of all estimates based on various approaches decrease as sample size grows (see Figures 2 and 3**).**

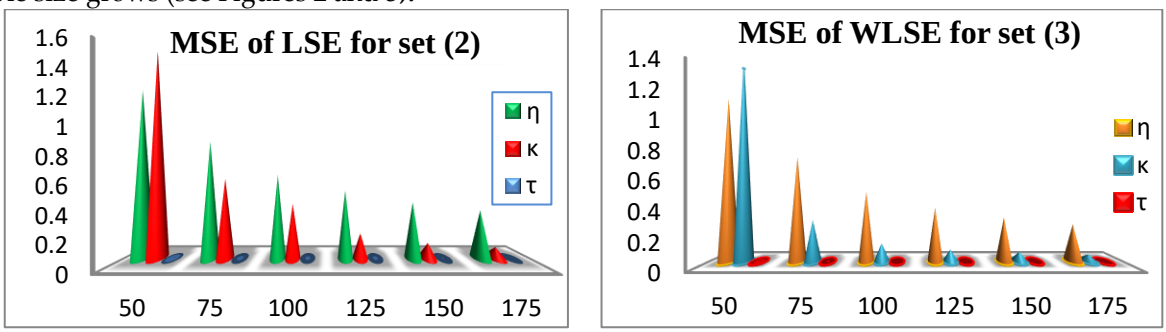

Figure 2: *The MSEs of the LSE and WLSE for the UPLoD for all values of m*

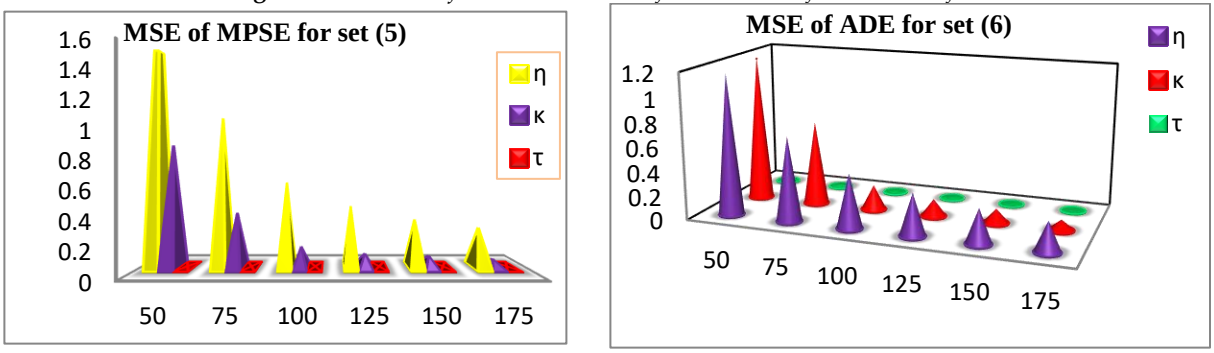

Figure 3: The MSEs of ADE and MPSE for the UPLoD for all values of *m*

7. It can be seen from Figure 4 that the MSE of κ estimates from AD and WLS methods gets the least value followed by the ML method compared to other methods for set 3 and set 4.

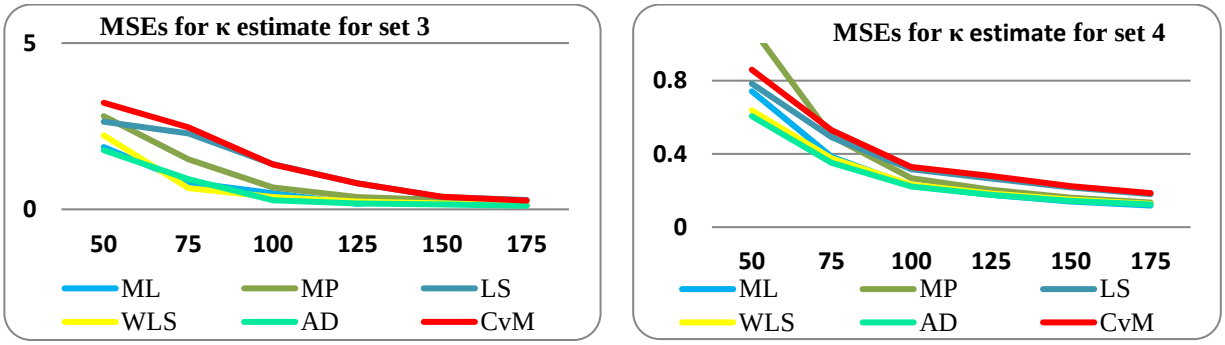

Figure 4: *The MSEs for different* κ *estimates of the UPLoD for all m values*

8. For sets 2 and 6, the MSE of η estimates based on the AD and WLS techniques yields the lowest values, followed by the ML approach in comparison to other methods (see Figure (5)).

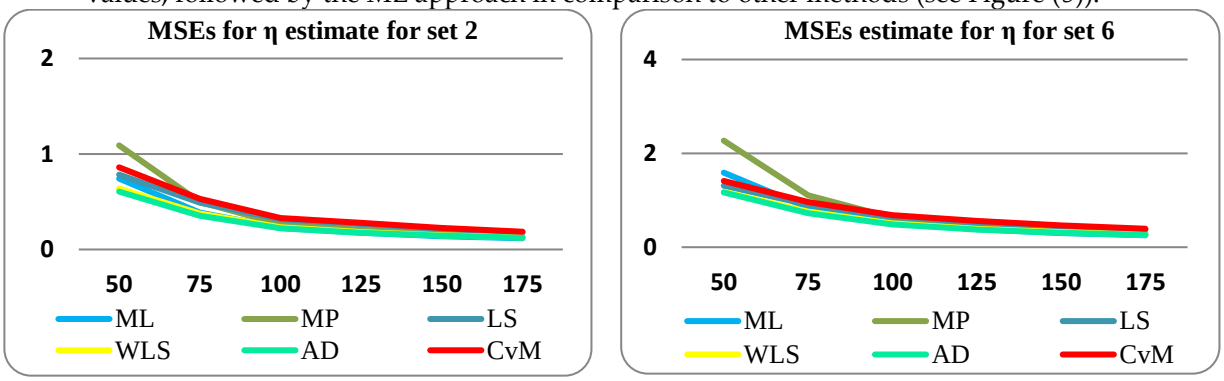

Figure 5: *The MSEs of different* η *estimates of the UPLoD for all values of m*

Table 3: *MSEs and RABs of different estimates for* $\eta = 2$, $\kappa = 0.8$, $\tau = 0.05$

m		ML		MP		LS		WLS		AD		CvM	
		MSE	RAB	MSE	RAB	MSE	RAB	MSE	RAB	MSE	RAB	MSE	RAB
50	η	0.425	0.074	0.586	0.129	0.369	0.046	0.0339	0.004	0.333	0.059	0.402	0.073
	κ	1.872	0.436	2.803	0.607	2.635	0.476	2.226	0.443	1.777	0.408	3.206	0.545
	τ	0.001	1.276	0.002	1.303	0.001	1.362	0.002	1.449	0.001	1.36	0.001	1.226
75	η	0.227	0.049	0.291	0.085	0.259	0.045	0.216	0.039	0.212	0.048	0.272	0.64
	κ	0.81	0.252	1.507	0.363	2.286	0.433	0.641	0.216	0.911	0.228	2.466	0.419
	τ	0.0009	1.067	0.0009	1.025	0.001	1.188	0.001	1.014	0.001	0.944	0.001	1.15
100	η	0.144	0.034	0.171	0.06	0.184	0.035	0.146	0.028	0.14	0.035	0.197	0.049
	κ	0.481	0.172	0.658	0.243	1.363	0.287	0.368	0.151	0.268	0.125	1.349	0.294
	τ	0.0007	0.845	0.0007	0.827	0.0011	1.093	0.0008	0.905	0.0007	0.792	0.0011	1.031
125	η	0.109	0.029	0.125	0.049	0.153	0.031	0.114	0.024	0.109	0.03	0.159	0.043
	κ	0.171	0.108	0.367	0.169	0.779	0.214	0.23	0.115	0.179	0.095	0.781	0.223
	τ	0.0005	0.673	0.0005	0.671	0.0009	0.971	0.0006	0.742	0.0005	0.654	0.0009	0.923
150	η	0.087	0.021	0.099	0.039	0.127	0.025	0.093	0.019	0.089	0.023	0.133	0.034
	κ	0.38	0.112	0.286	0.145	0.368	0.159	0.172	0.097	0.149	0.084	0.376	0.166
	τ	0.0003	0.552	0.0004	0.544	0.0009	0.947	0.0004	0.617	0.0003	0.526	0.0008	0.905
175	η	0.073	0.019	0.083	0.033	0.109	0.023	0.079	0.018	0.078	0.021	0.114	0.031
	κ	0.13	0.077	0.153	0.108	0.281	0.117	0.123	0.068	0.107	0.061	0.264	0.12
	τ	0.0003	0.455	0.0003	0.439	0.0006	0.728	0.0003	0.492	0.0003	0.432	0.0006	0.713

Table 4: *MSEs and RABs of different estimates for* $\eta = 2.5$, $\kappa = 0.8$, $\tau = 0.05$

m		ML		MP		LS		WLS		AD		CvM	
		MSE	RAB	MSE	RAB	MSE	RAB	MSE	RAB	MSE	RAB	MSE	RAB
50	η	0.742	0.079	1.09	0.14	0.784	0.064	0.638	0.052	0.606	0.066	0.86	0.095
	κ	1.883	0.45	2.249	0.563	1.941	0.419	1.297	0.369	1.209	0.362	2.36	0.47
	τ	0.026	1.082	0.031	1.189	0.03	1.205	0.027	1.127	0.027	1.139	0.03	1.151
75	η	0.385	0.053	0.497	0.09	0.491	0.054	0.376	0.042	0.352	0.049	0.529	0.074
	κ	0.495	0.215	1.342	0.356	1.43	0.326	0.738	0.217	0.695	0.211	1.421	0.336
	τ	0.018	0.084	0.018	0.807	0.018	0.84	0.017	0.794	0.017	0.763	0.019	0.826
100	η	0.226	0.034	0.267	0.06	0.317	0.038	0.232	0.029	0.222	0.036	0.328	0.052
	κ	0.479	0.172	0.716	0.246	1.309	0.279	0.368	0.151	0.268	0.125	1.242	0.282
	τ	0.011	0.621	0.012	0.632	0.015	0.738	0.012	0.623	0.011	0.577	0.015	0.715
125	η	0.176	0.031	0.204	0.052	0.266	0.035	0.183	0.025	0.176	0.031	0.28	0.046
	κ	0.279	0.113	0.235	0.148	0.461	0.179	0.174	0.103	0.141	0.087	0.49	0.189
	τ	0.007	0.447	0.008	0.485	0.015	0.722	0.009	0.524	0.008	0.444	0.015	0.702
150	η	0.139	0.022	0.161	0.041	0.216	0.027	0.15	0.019	0.144	0.024	0.224	0.036
	κ	0.194	0.097	0.189	0.127	0.264	0.14	0.133	0.088	0.118	0.077	0.274	0.147
	τ	0.006	0.386	0.006	0.389	0.011	0.619	0.007	0.44	0.006	0.388	0.011	0.584
175	η	0.118	0.019	0.134	0.035	0.18	0.025	0.127	0.018	0.124	0.022	0.186	0.033
	κ	0.097	0.07	0.115	0.096	0.195	0.102	0.096	0.062	0.086	0.056	0.199	0.107
	τ	0.005	0.311	0.005	0.318	0.008	0.469	0.005	0.327	0.004	0.293	0.008	0.456

Table 5: *MSEs and RABs of different estimates for* $\eta = 3$, $\kappa = 0.67$, $\tau = 0.05$

m		ML		MP		LS		WLS		AD		CvM	
		MSE	RAB	MSE	RAB	MSE	RAB	MSE	RAB	MSE	RAB	MSE	RAB
50	η	1.187	0.089	1.661	0.154	0.959	0.051	0.873	0.048	0.851	0.064	1.065	0.082
	κ	0.726	0.325	0.905	0.427	1.201	0.416	1.566	0.431	0.549	0.288	1.306	0.443
	τ	0.002	1.393	0.002	1.355	0.002	1.497	0.002	1.509	0.001	1.386	0.002	1.438
75	η	0.607	0.059	0.802	0.103	0.671	0.051	0.552	0.043	0.536	0.05	0.712	0.071
	κ	0.328	0.174	0.402	0.237	0.699	0.279	0.301	0.169	0.237	0.152	0.797	0.304
	τ	0.0009	1.009	0.0009	0.902	0.001	1.154	0.0009	1.075	0.0008	0.938	0.001	1.088
100	η	0.379	0.042	0.463	0.074	0.474	0.039	0.367	0.031	0.358	0.039	0.501	0.054
	κ	0.136	0.112	0.152	0.141	0.267	0.161	0.131	0.104	0.104	0.089	0.285	0.173
	τ	0.0006	0.776	0.0006	0.691	0.0009	0.995	0.0007	0.842	0.0006	0.757	0.0009	0.943
125	η	0.282	0.035	0.334	0.06	0.394	0.036	0.287	0.027	0.275	0.032	0.413	0.047
	κ	0.09	0.08	0.099	0.104	0.195	0.131	0.086	0.079	0.076	0.069	0.202	0.139
	τ	0.0005	0.62	0.0004	0.569	0.0009	0.962	0.0006	0.723	0.0005	0.626	0.0009	0.936
150	η	0.221	0.026	0.26	0.047	0.319	0.028	0.234	0.021	0.225	0.025	0.336	0.038
	κ	0.073	0.072	0.082	0.092	0.119	0.104	0.069	0.069	0.063	0.062	0.123	0.109
	τ	0.0003	0.494	0.0003	0.462	0.0007	0.831	0.0004	0.579	0.0003	0.511	0.0006	0.795
175	η	0.186	0.022	0.216	0.041	0.279	0.027	0.198	0.019	0.194	0.023	0.288	0.034
	κ	0.049	0.053	0.057	0.069	0.088	0.074	0.051	0.048	0.047	0.045	0.089	0.079
	τ	0.0003	0.428	0.0003	0.388	0.0005	0.676	0.0003	0.478	0.0003	0.437	0.0005	0.647

Table 6: *MSEs and RABs of different estimates for* $\eta = 3.5$, $\kappa = 0.67$, $\tau = 0.05$

m		ML		MP		LS		WLS		AD		CvM	
		MSE	RAB	MSE	RAB	MSE	RAB	MSE	RAB	MSE	RAB	MSE	RAB
50	η	1.589	0.089	2.271	0.153	1.31	0.052	1.182	0.048	1.168	0.068	1.412	0.079
	κ	0.729	0.325	0.904	0.426	1.623	0.464	1.493	0.418	0.549	0.288	1.674	0.487
	τ	0.002	1.393	0.002	1.353	0.002	1.498	0.002	1.509	0.001	1.386	0.002	1.438
75	η	0.84	0.06	1.106	0.103	0.909	0.051	0.761	0.043	0.725	0.052	0.966	0.07
	κ	0.328	0.174	0.403	0.237	0.62	0.27	0.301	0.168	0.237	0.152	0.775	0.302
	τ	0.0009	1.009	0.0008	0.903	0.001	1.153	0.0009	1.075	0.0009	0.957	0.001	1.088
100	η	0.516	0.042	0.629	0.074	0.647	0.039	0.506	0.031	0.482	0.038	0.686	0.055
	κ	0.136	0.112	0.152	0.141	0.424	0.179	0.131	0.104	0.104	0.089	0.385	0.187
	τ	0.0006	0.775	0.0006	0.692	0.0009	0.996	0.0007	0.842	0.0006	0.757	0.0009	0.943
125	η	0.383	0.035	0.454	0.06	0.528	0.036	0.389	0.027	0.376	0.033	0.56	0.047
	κ	0.09	0.08	0.099	0.104	0.195	0.131	0.086	0.079	0.076	0.069	0.202	0.139
	τ	0.0005	0.62	0.0005	0.588	0.0009	0.963	0.0006	0.723	0.0005	0.626	0.0009	0.936
150	η	0.302	0.026	0.354	0.047	0.436	0.028	0.319	0.021	0.307	0.025	0.462	0.038
	κ	0.073	0.072	0.082	0.092	0.119	0.104	0.069	0.069	0.063	0.062	0.123	0.109
	τ	0.0003	0.494	0.0003	0.462	0.0007	0.831	0.0004	0.579	0.0003	0.511	0.0006	0.795
175	η	0.254	0.023	0.293	0.041	0.374	0.026	0.269	0.019	0.264	0.023	0.394	0.034
	κ	0.049	0.053	0.057	0.069	0.087	0.074	0.051	0.048	0.047	0.045	0.089	0.079
	τ	0.0003	0.428	0.0003	0.388	0.0005	0.676	0.0003	0.478	0.0003	0.437	0.0005	0.647

Table 7: MSEs and RABs of different estimates for $\eta = 3$, $\kappa = 0.8$, $\tau = 0.05$

m		ML		MP		LS		WLS		AD		CvM	
		MSE	RAB	MSE	RAB	MSE	RAB	MSE	RAB	MSE	RAB	MSE	RAB
50	η	1.074	0.079	1.617	0.141	1.122	0.064	0.914	0.052	0.861	0.066	1.24	0.095
	κ	1.885	0.451	2.241	0.563	1.9	0.411	1.296	0.369	0.899	0.453	2.247	0.471
	τ	0.026	1.082	0.031	1.189	0.03	1.204	0.027	1.127	0.098	1.046	0.0301	1.151
75	η	0.549	0.052	0.707	0.089	0.712	0.054	0.546	0.042	0.499	0.049	0.747	0.073
	κ	0.495	0.215	1.345	0.356	1.429	0.326	0.739	0.217	0.695	0.211	1.438	0.339
	τ	0.018	0.84	0.018	0.807	0.018	0.84	0.017	0.794	0.017	0.763	0.019	0.837
100	η	0.337	0.036	0.402	0.063	0.471	0.039	0.344	0.029	0.329	0.036	0.498	0.054
	κ	0.282	0.148	0.416	0.209	0.857	0.24	0.374	0.146	0.205	0.113	0.77	0.241
	τ	0.011	0.615	0.01	0.579	0.014	0.701	0.011	0.604	0.01	0.55	0.014	0.678
125	η	0.253	0.031	0.293	0.051	0.384	0.035	0.264	0.025	0.253	0.031	0.404	0.046
	κ	0.279	0.113	0.235	0.148	0.461	0.179	0.174	0.103	0.141	0.087	0.491	0.189
	τ	0.007	0.447	0.009	0.504	0.015	0.722	0.009	0.524	0.008	0.444	0.015	0.603
150	η	0.201	0.002	0.231	0.041	0.31	0.027	0.216	0.019	0.208	0.024	0.328	0.037
	κ	0.194	0.097	0.188	0.128	0.264	0.14	0.133	0.088	0.118	0.077	0.274	0.147
	τ	0.006	0.386	0.006	0.39	0.011	0.619	0.007	0.44	0.006	0.388	0.011	0.584
175	η	0.169	0.019	0.193	0.035	0.259	0.025	0.183	0.018	0.179	0.022	0.269	0.033
	κ	0.097	0.07	0.115	0.096	0.195	0.102	0.096	0.062	0.086	0.056	0.199	0.107
	τ	0.005	0.311	0.005	0.318	0.008	0.469	0.004	0.327	0.004	0.293	0.008	0.456

Table 8: *MSEs and RABs of different estimates for* $\eta = 3.5$, $\kappa = 0.8$, $\tau = 0.05$

m		ML		MP		LS		WLS		AD		CvM	
		MSE	**RAB**	**MSE**	**RAB**	**MSE**	**RAB**	**MSE**	**RAB**	**MSE**	**RAB**	**MSE**	**RAB**
50	η	1.462	0.079	2.179	0.141	1.521	0.064	1.233	0.051	1.164	0.065	1.698	0.095
	κ	1.888	0.451	2.242	0.563	1.958	0.42	1.297	0.369	1.215	0.362	2.245	0.471
	τ	0.026	1.082	0.029	1.171	0.03	1.205	0.027	1.127	0.027	1.139	0.03	1.151
75	η	0.745	0.052	0.969	0.089	0.984	0.055	0.739	0.042	0.696	0.05	1.028	0.073
	κ	0.495	0.215	1.347	0.356	1.432	0.326	0.733	0.216	0.695	0.221	1.433	0.339
	τ	0.018	0.84	0.018	0.807	0.018	0.84	0.017	0.794	0.017	0.762	0.0195	0.837
100	η	0.459	0.036	0.547	0.063	0.638	0.039	0.468	0.029	0.447	0.036	0.681	0.054
	κ	0.282	0.148	0.414	0.209	0.858	0.241	0.375	0.146	0.205	0.113	0.769	0.241
	τ	0.011	0.616	0.01	0.58	0.014	0.701	0.011	0.604	0.01	0.55	0.014	0.678
125	η	0.344	0.031	0.399	0.052	0.517	0.034	0.359	0.025	0.346	0.031	0.538	0.046
	κ	0.279	0.113	0.237	0.148	0.461	0.179	0.174	0.103	0.141	0.087	0.49	0.189
	τ	0.007	0.447	0.008	0.485	0.015	0.722	0.009	0.524	0.008	0.444	0.014	0.602
150	η	0.274	0.022	0.315	0.041	0.415	0.027	0.294	0.019	0.282	0.024	0.438	0.036
	κ	0.194	0.097	0.188	0.182	0.264	0.14	0.133	0.088	0.118	0.077	0.274	0.147
	τ	0.006	0.386	0.006	0.39	0.011	0.619	0.007	0.44	0.006	0.388	0.011	0.584
175	η	0.231	0.019	0.262	0.035	0.354	0.025	0.248	0.018	0.244	0.022	0.368	0.033
	κ	0.097	0.07	0.115	0.096	0.195	0.102	0.096	0.062	0.087	0.056	0.199	0.107
	τ	0.005	0.311	0.005	0.318	0.008	0.469	0.005	0.327	0.004	0.293	0.008	0.456

6 Applications to Real Data

In this section, a data analysis is provided in order to examine the goodness-of-fit of the UPLoD when compared to some other models, namely UWD, ULD, UGoD, ULLD, UBXIID, UG/GD, Kumaraswamy distribution (KumD) (Kumaraswamy [35]) and Toppe-Leone distribution (TLD) (Nadarajah and Kotz [36]).

i. First Data Set

The first real data set represents 20 observations of comprised water capacity month-wise from the Shasta reservoir in California in the month of February from 1991-2010. Hashmi *et al.* [20] provided the dataset. The following are the data details

0.0833	0.0833	0.1167	0.1167	0.1167	0.15	0.1833	0.2167	0.2167
0.25	0.25	0.25	0.25	0.2833	0.3167	0.35	0.3833	0.4167
0.4167	0.45	0.4833	0.4833	0.7167	0.7167	0.75	0.75	0.85
0.9167								

Some of the data's values can be summarized as follows: Q_1 =0.208, Q_2 =0.300, Q_3 =0.483, mean=0.377, $\alpha_3 = 0.765$, and $\alpha_4 = 2.421$. The MLEs and standard errors (SEs) for all models are given in Table 9. The measures of fit statistic using the maximized log-likelihood (-2logL), Akaike information criterion (E_1), Bayesian information criterion (E_2), the correct Akaike information criterion (E_3), Hannan-Quinn information criterion (E_4), the Kolmogorov Smirnov (KS) statistic values along with P-value, CvM test (CvMT) and AD test (ADT) are calculated in Table 9. The model with minimum values for -2logL, E_1, E_2, E_3 and E_4 can be selected as the model that best fits the data.

Table 9: *MLEs and SEs of all model parameters for the first data*

	Models					
	UBXIID	**UG/GD**	**UPLoD**	**UWD**	**KumD**	**TLD**
κ	1.765	28.097	3.833	1.57	—	—
SE	(0.254)	(8.125)	(0.427)	(0.248)		
η	5.856	0.168	0.589	4.207	4.489	—
SE	(1.549)	(0.069)	(0.165)	(1.12)	(2.041)	
τ	—	63.538	0.003	—	6.347	0.867
SE		(67.518)	(0.002)		(1.558)	(1.938)

Table 10: *The statistical measures for the first data*

Measures	**Models**					
	UBXIID	**UG/GD**	**UPLoD**	**UWD**	**KumD**	**TLD**
-2log L	-11.744	-15.366	-16.272	-10.957	-13.475	-11.587
E_1	-19.488	-24.732	-26.543	-17.914	-22.949	-21.175
E_2	-17.497	-21.744	-23.556	-15.922	-20.958	-20.179
E_3	-18.783	-24.149	-25.043	-17.208	-22.244	-20.953
E_4	-19.099	-24.149	-25.96	-17.525	-22.561	-20.981
KS	0.225	0.192	0.1504	0.242	0.221	0.255
P-value	0.224	0.399	0.701	0.1638	0.245	0.124
CvMT	0.295	0.174	0.105	0.332	0.241	0.313
ADT	1.701	1.081	0.726	1.874	1.425	1.786

The results show that the UPLoD provides a significantly more suited compared to the other five models. The left panel of Figure 6 shows that the box plots is left-skewed. Also, the right panel of Figure 6 shows that the total time on test (TTT) plot is concave; that is, TTT plot was obtained and compared the hazard line, which is an increasing function. Figure 7 shows the probability-probability (PP) plots, also referred to as "parametric plots," and the CDF line empirically (red) utilizing the projected CDF line (black) of the UPLoD of monthly water capacity from the Shasta reservoir in California for the month of February from 1991 to 2010 to illustrate the empirical findings reported in Table 10.

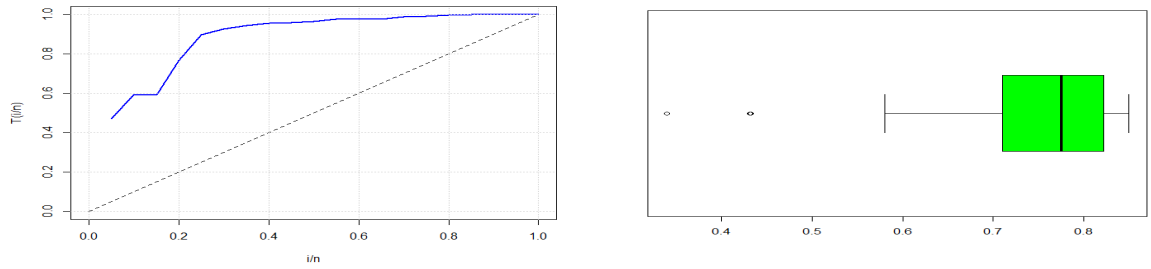

Figure 6: *Boxplot and TTT plots of the UPLoD for the first data*

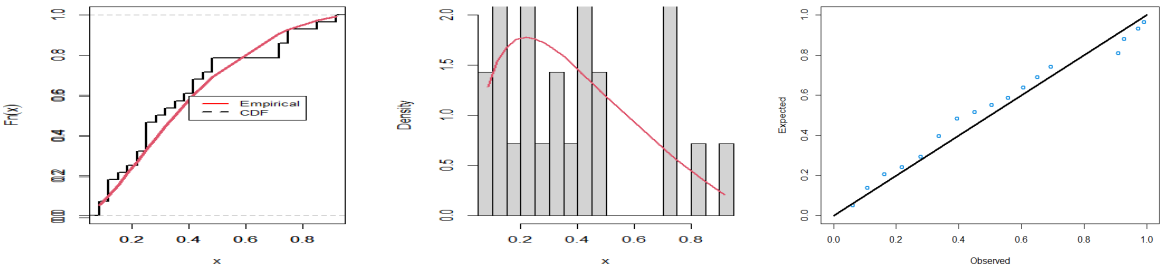

Figure 7: *The CDF plot with line empirically, fitted PDF and PP plots for the first data*

ii. Second Data Set

The second data set represents 20 observations of the maximum flood level (in millions of cubic feet per second) for the Susquehanna River at Harrisburg, Pennsylvania. The data set was taken from Mazucheli *et al.* [8]. The data are as below:

0.26	0.27	0.3	0.32	0.32	0.34	0.38	0.38	0.39	0.4
0.41	0.42	0.42	0.42	0.45	0.48	0.49	0.61	0.65	0.74

Here's a summary of some of the data's values: Q_1 =0.335, Q_2 =0.405, Q_3 =0.458, mean=0.423, $\alpha_3 = 1.07$, and $\alpha_4 = 3.66$. The MLEs and SEs for all models are given in Table 11. The measures of fit are calculated in Table 12. The model with minimum values for the proposed measures can be chosen as the best model to fit the data.

Table 11: *MLEs and SEs of all model parameters for the second data*

	Models					
	UBXIID	**ULLD**	**UG/GD**	**UPLoD**	**KumD**	**TLD**
κ	1.646	5.274	4.021	3.967	12.005	—
SE	(0.37)	(1.023)	(1.134)	(0.741)	(5.474)	
η	4.848	—	2.019	27.109	3.377	—
SE	(0.918)		(1.859)	(70.70)	(0.604)	
τ	—	0.894	76.349	25.757	—	2.241
SE		(0.064)	(48.889)	(68.84)		(0.501)

Table 12: *The statistical measures for the second data*

Measures	**Models**					
	UBXIID	**ULLD**	**UG/GD**	**UPLoD**	**KumD**	**TLD**
-2log L	-14.747	-13.853	-15.162	-16.100	-12.973	-7.381
E_1	-25.494	-23.707	-24.324	-26.200	-21.241	-12.763
E_2	-23.102	-21.715	-21.337	-23.213	-21.241	-11.767
E_3	-24.608	-23.007	-22.824	-24.700	-21.132	-12.541
E_4	-25.105	-23.318	-23.741	-25.617	-21.558	-12.568
KS	0.1882	0.1604	0.204	0.147	0.2175	0.3409
P-value	0.4777	0.6823	0.374	0.781	0.3005	0.0191
CvMT	0.0930	0.1197	0.061	0.059	0.1673	0.1195
ADT	0.5765	0.7323	0.29	0.353	0.9747	0.7111

The results show that the UPLoD provides a significantly more suited compared to the other five models. The left panel of Figure 8 shows that the box plots is right skewed. Also, the right panel of Figure 8 shows that the TTT plot is concave. Figure 9 illustrates the empirical finding given in Table 12 by showing

the PP plots, and the CDF line empirically (red) utilizing the projected CDF line (black), for the UPLoD of the maximum flood level cubic feet per for the Susquehanna River.

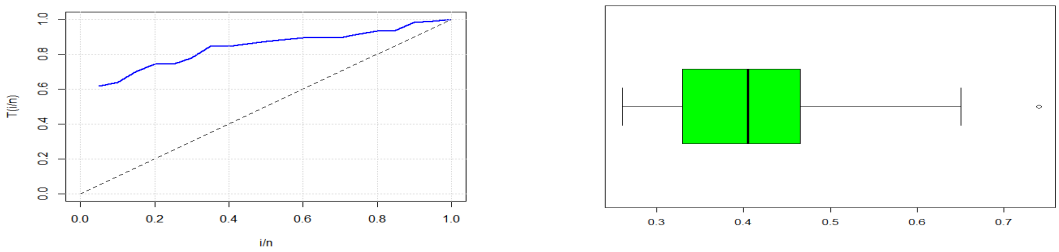

Figure 8: *Boxplot and TTT plot of the UPLoD for the second data*

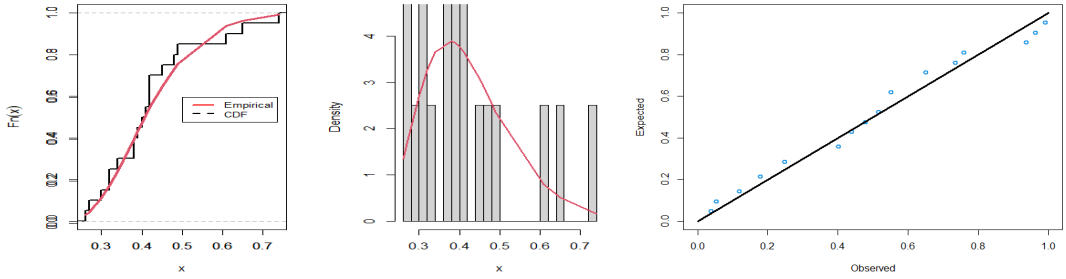

Figure 9: *The CDF plot with line empirically, fitted PDF and PP plots employing the second data*

7 Conclusion

We offer a new bounded distribution in this study, which we term the unit power Lomax distribution, as an alternative to several new bounded distributions. The UPLoD captures several kinds of density and hazard functions. Moments, incomplete moments, PWM, residual and inverted residual lives, quantile function, and entropy measurements are some of the mathematical characteristics of the proposed UPLoD. Some metrics of entropy have also been determined. The unknown parameters of the proposed UPLoD are estimated using the ML, LS, CvM, WLS, AD, and MPS techniques. The asymptotic behaviour of the parameter estimates for the UPLoD was investigated using a simulated study. The findings of the simulation indicate that the WLS and AD approaches are better than the others. Two real-data examples demonstrate that the UPLoD outperforms all competitors in fitting this type of data set.

Funding: No funding was received for this work.
Conflicts of Interest: The authors declare that they have no conflicts of interest.

References

[1] Lomax, K.S. (1954), Business failures: Another example of the analysis of failure data. *Journal of the American statistical association*, **49**(268): 847–852

[2] Harris, C.M. (1968), The Pareto distribution as a queue service discipline. *Operations Research*, **16**(2): 307–313

[3] Bryson, M.C. (1974), Heavy-tailed distributions: properties and tests. *Technometrics*, **16**(1): 61–68

[4] Atkinson, A.B. and Harrison, A.J. (1978), Distribution of personal wealth in Britain. *The Economic Journal*, **88**(351): 581–583

[5] Holland, O., Golaup, A., and Aghvami, A.H. (2006), Traffic characteristics of aggregated module downloads for mobile terminal reconfiguration. *IEE Proceedings-Communications*, **153**(5): 683–690

[6] Rady, E.-H.A., Hassanein, W.A., and Elhaddad, T.A. (2016), The power Lomax distribution with an application to bladder cancer data. *SpringerPlus*, **5**: 1–22

[7] Gómez-Déniz, E., Sordo, M.A., and Calderín-Ojeda, E. (2014), The Log–Lindley distribution as an alternative to the beta regression model with applications in insurance. *Insurance: Mathematics and Economics*, **54**: 49–57

[8] Mazucheli, J., Menezes, A.F., and Dey, S. (2019), Unit-Gompertz distribution with applications. *Statistica*, **79**(1): 25–43

[9] Mazucheli, J., Menezes, A.F.B., and Chakraborty, S. (2019), On the one parameter unit-Lindley distribution and its associated regression model for proportion data. *Journal of Applied Statistics*, **46**(4): 700–714

[10] Haq, M.A.u., Hashmi, S., Aidi, K., Ramos, P.L., and Louzada, F. (2020), Unit modified Burr-III distribution: Estimation, characterizations and validation test. *Annals of Data Science*: 1–26

[11] Korkmaz, M.Ç. (2020), The unit generalized half normal distribution: A new bounded distribution with inference and application. *UPB Scientific Bulletin, Series A: Applied Mathematics and Physicsopen access*, **82**(2): 133–140

[12] Mazucheli, J., Menezes, A.F.B., Fernandes, L.B., De Oliveira, R.P., and Ghitany, M.E. (2020), The unit-Weibull distribution as an alternative to the Kumaraswamy distribution for the modeling of quantiles conditional on covariates. *Journal of Applied Statistics*, **47**(6): 954–974

[13] Bantan, R.A.R., Jamal, F., Chesneau, C., and Elgarhy, M. (2021), Theory and applications of the unit gamma/Gompertz distribution. *Mathematics*, **9**(16): 1850. https://doi.org/10.3390/math9161850

[14] Ribeiro-Reis, L.D. (2021), Unit log-logistic distribution and unit log-logistic regression model. *Journal of the Indian Society for Probability and Statistics*, **22**(2): 375–388

[15] Korkmaz, M.Ç. and Chesneau, C. (2021), On the unit Burr-XII distribution with the quantile regression modeling and applications. *Computational and Applied Mathematics*, **40**(1): 29. https://doi.org/10.1007/s40314-021-01418-5

[16] Ramadan, A.T., Tolba, A.H., and El-Desouky, B.S. (2022), A unit half-logistic geometric distribution and its application in insurance. *Axioms*, **11**(12): 676. https://doi.org/10.3390/axioms11120676

[17] Martínez-Flórez, G., Azevedo-Farias, R.B., and Tovar-Falón, R. (2022), New class of unit-power-skew-normal distribution and its associated regression model for bounded responses. *Mathematics*, **10**(17): 3035

[18] Hassan, A.S., Fayomi, A., Algarni, A., and Almetwally, E.M. (2022), Bayesian and non-Bayesian inference for unit-exponentiated half-logistic distribution with data analysis. *Applied Sciences*, **12**(21): 11253. https://doi.org/10.3390/app122111253

[19] Krishna, A., Maya, R., Chesneau, C., and Irshad, M.R. (2022), The unit Teissier distribution and its applications. *Mathematical and Computational Applications*, **27**(1): 12. https://doi.org/10.3390/mca27010012

[20] Hashmi, S., Ahsan-ul-Haq, M., Zafar, J., and Khaleel, M.A. (2022), Unit Xgamma distribution: its properties, estimation and application: Unit-Xgamma distribution. *Proceedings of the Pakistan Academy of Sciences: A. Physical and Computational Sciences*, **59**(1): 15–28

[21] Haj Ahmad, H., Almetwally, E.M., Elgarhy, M., and Ramadan, D.A. (2023), On unit exponential pareto distribution for modeling the recovery rate of COVID-19. *Processes*, **11**(1): 232. https://doi.org/10.3390/pr11010232

[22] Fayomi, A., Hassan, A.S., and Almetwally, E.M. (2023), Inference and quantile regression for the unit-exponentiated Lomax distribution. *Plos one*, **18**(7): e0288635. https://doi.org/10.1371/journal.pone.0288635

[23] Akata, I.U., Opone, F.C., and Osagiede, F.E.U. (2023), The Kumaraswamy unit-Gompertz distribution and its application to lifetime datasets. *Earthline Journal of Mathematical Sciences*, **11**(1): 1–22

[24] Hassan, A.S. and Alharbi, R.S. (2023), Different estimation methods for the unit inverse exponentiated Weibull distribution. *Communications for Statistical Applications and Methods*, **30**(2): 191–213

[25] Fayomi, A., Hassan, A.S., Baaqeel, H., and Almetwally, E.M. (2023), Bayesian inference and data analysis of the unit-power Burr X distribution. *Axioms*, **12**(3): 297. https://doi.org/10.3390/axioms12030297

[26] Greenwood, J.A., Landwehr, J.M., Matalas, N.C., and Wallis, J.R. (1979), Probability weighted moments: definition and relation to parameters of several distributions expressable in inverse form. *Water Resources Research*, **15**(5): 1049–1054

[27] Balkema, A.A. and De Haan, L. (1974), Residual life time at great age. *The Annals of Probability*, **2**(5): 792–804

[28] Havrda, J. and Charvát, F. (1967), Quantification method of classification processes. Concept of structural-entropy. *Kybernetika*, **3**(1): 30–35

[29] Tsallis, C. (1988), Possible generalization of Boltzmann-Gibbs statistics. *Journal of Statistical Physics*, **52**(1): 479–487

[30] Arimoto, S. (1971), Information-theoretical considerations on estimation problems. *Information and Control*, **19**(3): 181–194

[31] Hassan, A.S., Elshaarawy, R., and Nagy, H.F. (2023), Reliability analysis of exponentiated exponential distribution for neoteric and ranked sampling designs with applications. *Statistics, Optimization & Information Computing*, **11**(3): 580–594

[32] Hassan, A.S., Ismail, D.M., and Nagy, H.F. (2023), Analysis of a non-identical component-strengths system based on lower record data. *Reliability: Theory & Applications*, **18**(2 (73)): 513–528

[33] Hassan, A.S., Elshaarawy, R., and Nagy, H.F. (2024), Estimation Study of Multicomponent Stress-Strength Reliability Using Advanced Sampling Approach. *Gazi University Journal of Science*, **37**(1): 465–481

[34] Cheng, R.C.H. and Amin, N.A.K. (1979), Maximum product-of-spacings estimation with applications to the lognormal distribution. *University of Wales IST: Cardiff, UK, Mathematical Report*, **79-1**

[35] Kumaraswamy, P. (1980), A generalized probability density function for double-bounded random processes. *Journal of Hydrology*, **46**(1-2): 79–88

[36] Nadarajah, S. and Kotz, S. (2003), Moments of some J-shaped distributions. *Journal of Applied Statistics*, **30**(3): 311–317